Radiation and Mixed Convection Effects on Chemically Reactive Sisko Fluid Flow over a Curved Stretching Surface

Ahmad, Latif*[+•]

Department of Mathematics, Quaid-i-Azam University, Islamabad 44000, PAKISTAN

Alshomrani, Ali Saleh

Department of Mathematics Shaheed Benazir Bhutto University, Sheringal Dir Upper 180000, PAKISTAN

Khan, Masood

NAAM Research Group, Department of Mathematics, Faculty of Science, King Abdulaziz University, Jeddah 21589, SAUDI ARABIA

ABSTRACT: *The main objective of this framework is to establish the modeling and simulation of mixed convection flows along with a curved stretching sheet with Sisko fluid. The impacts of thermal radiation and first-order chemical reaction are also incorporated to illustrate the heat and mass transfer phenomenon. In addition, the convective condition is deliberated to discuss the heat transfer mechanism. The normalized conservation equations emerge as a system of non-linear two-dimensional coupled Partial Differential Equations (PDEs). Under appropriate transformation, these equations are converted into Ordinary Differential Equations (ODEs). Numerical procedures are examined in this study for various active parameters. A significant declining behavior of the velocity profile is depicted with an increase in mixed convection and buoyancy ratio parameter. An enhancement conduct in the temperature of the fluid is reported through the growing values of radiation parameter and Biot number. A remarkable decreasing trend is addressed by the higher values of the chemical reaction parameter while plotting the concentration profile of the fluid. Moreover, the resistive forces, heat, and mass transfer rates are discussed in tabular form. A comparison with shooting and RK-45 Fehlberg method is illustrated to show the validity of the present scheme. Thus the present consequences are well correlated with the existing literature.*

KEYWORDS: *Sisko fluid, mixed convection; Chemical reaction; Curved stretching; Numerical solutions; Curvilinear coordinates.*

* *To whom correspondence should be addressed.*

+ *E-mail: latifahmad@math.qau.edu.pk*

• *Other Address: Department of Mathematics Shaheed Benazir Bhutto University, Sheringal Dir Upper 180000, PAKISTAN*

1021-9986/2020/4/339-354 16/$/6.06

INTRODUCTION

demise. A large number of studies [1-5] are carried out to explore the features of thermal radiation on flow and heat transfer. These types of flows are affected by the external agencies on the rate of flow and heat transfer. *Krishnamurthy et al.* [6] reported the effect of chemical reaction and thermal radiation on boundary layer slip flow and melting heat transfer of nano-liquid due to nonlinear stretched surface. Motsumi and Makinde [7] addressed the effects of viscous dissipation and radiation on boundary layer flow of nano-fluids over a permeable moving flat plate. *Hayat et al*. [8] illustrated the Soret and Dufour effects on the radiative 3D fluid flow. Moreover, the reactive hydro-magnetic heat producing liquid flow with thermal radiation inside porous channel with symmetrical convective cooling is elucidated by *Hassan et al.* [9].

Mixed convection spectacle is of huge significance since flow is driven affected by double forces. Mixed convection is wanted when just the forced convection or the natural convection is not adequate to accomplish the outcomes. The relative commitment of natural or forced convection relies on the flow conduct (laminar flow or turbulent flow) and temperature of the liquid. Mixed convection occurrence has uses in a few modern and designing procedures like water transportation framework, chilling of reactors, cooling frameworks, electronic gadgets cooling process and synthetic partition instruments. The skin sweating and vasodilatation in variable atmosphere circumstances are bolstered by radiation and mixed convection. At the point when surroundings temperature is not as much as that of body temperature, the body can go through heat over conduction and radiation. In this regard, *Sparrow et al.* [10] built up the comparability solution for the mixed convective boundary layer flow. Later on many researchers [11-15] attempted such phenomenal work to explore the impacts of gravity in fluid flow problems. Other than this, the concurrent results of thermal radiation and mixed convection is of prime hugeness in human physiology organs especially in brain, heart, liver and in tightening of skeletal muscles. Mixed convection flow along the vertical surface is considered to obtain the similarity solution when the free stream velocity is uniform which was discussed by *Merkin* and *Pop* [16]. *Nadeem* and *Saleem* [17] explored the mixed convection effects on Eyring Powell liquid on the rotating frame. *Noor et al.* [18] demonstrated the micro-polar nano-liquid flow with the influence of micro-rotation in the presence of mixed convection phenomenon. *Haq et al.* [19] studied the mixed convection flow along a vertically heated surface. *Turkyilmazoglu* [20] described analytically the importance of MHD mixed convection flow of micropolar fluid over a cooled/heated deformable plate. Furthermore, *Turkyilmazoglu* [21] reported the analytical solutions of MHD mixed convection flow of a fluid over a nonlinear permeable stretching surface. Recently, Modeling of MHD and stagnation point flow of thixotropic fluid with non-uniform heat absorption/generation studied by *Hayat et al.* [22].

A step toward building of boundary layer flow characteristics without stretching surfaces is almost incomplete. Since this phenomenon is playing an important role in industries, metallurgical engineering process etc. Utilization of stretching phenomenon contains the most important physical properties, i.e., growing of crystals, glass blowing, drawing and paper production, aerodynamics extrusion of plastic sheet and fibers etc. To develop and design equipment and new machines with high rate of heating/cooling for which a lot of work is carried out by many engineers and scientists. *Crane* [23] is one of those who discussed the fluid flow over a stretching surface. Various attempts [24, 25] were made to demonstrate different physical features with Newtonian and non-Newtonian fluid flows due to linear and nonlinear stretching surfaces. But, the fluid flow due to curved stretching surface has been not deliberated appropriately. Examination of fluid flow concerning linear stretching of curved surface was firstly presented by *Sajid et al.* [26]. In the aforementioned work the authors described the impact of curvature inside the boundary layer flow over curved surface. *Abbas et al.* [27] discussed the flow and heat transfer analysis in the presence of magnetic field due to curved stretching surface. *Rosca* and *Pop* [28] reported the flow of unsteady Newtonian fluid over a curved stretching surface. Flow of Newtonian fluid along a nonlinear curved stretching surface was considered by *Sanni et al.* [29].

The word fluid flow today is a main them for industrialist, engineers, and scientists. Attraction towards fluid flow phenomenon is going to be very interesting. But the most important applications are about the flow of non-Newtonian fluid rather than viscous fluids. Though, the viscous fluids follows Newton's law of viscosity which is a direct relationship between shear stress

and shear rate. But there are a lot of fluids like shampoo, ketchup, paints and mud etc. have a nonlinear relationship between shear stress and shear rate. Because of this reason such types of fluids are categorized as non-Newtonian fluids. Recently, extensive attention has been grew by the flows of non-Newtonian liquids in fermentation, composite processing, bubble columns, boiling, plastic foam processing, bubble absorptions and so forth. Flow, heat and mass transfer in non-Newtonian liquids due to moving surfaces have broad applications in medicinal companies (i.e. pharmaceutical medicinal technology) production of paper and polyethylene, cooling of elastic sheets, polymer extrusion, fiber technology, food processing and numerous others studies by authors [31-37]. Moreover, these studies have a lot of deficiencies i.e., to describe the shear thinning and shear thickening liquid properties. In this regard, coupled of investigations are carries out by few researchers [38-40]. Specifically, *Ahmad et al.* [41] addressed the effect of nanoparticles and magnetic field in the flow of Sisko fluid over a bidirectional stretching surface. Where they observed a negligible effect of Brownian motion parameter on the temperature profile for the recommended revised relation. Recently, *Malik* and *Khan* [42] illustrated the effect of homogenous-heterogeneous reactions in the flow of Sisko fluid past a stretched cylinder.

The exploration of non-Newtonian liquids occufying a stretching surface is one of the substantial phenomenon during the preceding few eras. Due to this non-negligible importance, the present illustration is a step toward filling of such shortages. However, in this exploration the impact of mixed convection, thermal radiation and chemical reaction with convective boundary conditions in the flow, heat and mass transfer scrutiny is considered. Additionally, all the governing flow, heat and mass transfer equations are modeled in the curvilinear coordinate system. Numerical approach is used to display all the results in graphical form. Specially, flow pattern is discussed with the help of streamlines which shows a significance impacts of the sundry parameters. Present outcomes are verified with another numerical scheme, namely shooting method with RK-45 Fehlberg.

PROBLEM FORMULATION

The mixed convection incompressible Sisko fluid flow over a curved surface is considered. Thermal radiation and chemical reaction are utilized to perform a critical analysis about the heat and mass transfer mechanisms. Furthermore, the effect of convective condition is presented to address the convection process in the fluid flow. The flow diagram is coiled in a circle with radius of curvature R and stretched with velocity $U_w = cs$ along $s-$direction with fluid forming a boundary layer in $r-$direction (see Fig. 1). The surface shall be more curved for smaller values of R and shall be made flat for larger value of R. The temperature and concentration of the fluid are T_f and C_f while far away from the curved surface these are T_∞ and C_∞, respectively. For a steady flow, the governing equations [43] involving of the continuity, momentum, temperature and concentration equations, respectively, are illustrated in the curvilinear coordinate structure as:

$$\frac{\partial}{\partial r}\{(r+R)v\} + R\frac{\partial u}{\partial s} = 0, \tag{1}$$

$$\frac{u^2}{r+R} = \frac{1}{\rho}\frac{\partial p}{\partial r}, \tag{2}$$

$$\nu\frac{\partial u}{\partial r} + \frac{Ru}{r+R}\frac{\partial u}{\partial s} + \frac{\partial v}{r+R} = \tag{3}$$

$$-\frac{1}{\rho}\frac{R}{r+R}\frac{\partial p}{\partial s} + \frac{a}{\rho(r+R)^2}\frac{\partial}{\partial r}\left[(r+R)^2\left(\frac{\partial u}{\partial r} - \frac{u}{r+R}\right)\right] +$$

$$+\frac{b}{\rho(r+R)^2}\frac{\partial}{\partial r}\left[(r+R)^2\left(\frac{\partial u}{\partial r} - \frac{u}{r+R}\right)^n\right] +$$

$$g\beta_T(T - T_\infty) + g\beta_C(C - C_\infty)$$

$$\nu\frac{\partial T}{\partial r} + \frac{RU}{r+R}\frac{\partial T}{\partial s} = \tag{4}$$

$$\alpha_1\left(\frac{\partial^2 T}{\partial r^2} + \frac{1}{r+R}\frac{\partial T}{\partial r}\right) - \frac{1}{r+R}\frac{\partial}{\partial r}(r+R)q_r$$

$$\nu\frac{\partial C}{\partial r} + \frac{RU}{r+R}\frac{\partial C}{\partial s} = \tag{5}$$

$$D_B\left(\frac{\partial^2 C}{\partial r^2} + \frac{1}{r+R}\frac{\partial C}{\partial r}\right) - \vartheta(C - C_\infty)$$

Subjected to the following boundary conditions:

$$u = U_w(s) = cs,\ v = 0, \tag{6}$$
$$-k\frac{\partial T}{\partial r} = h_f(T_f - T),\ C = C_f \text{ at } r = 0,$$

$$u \to 0,\ \frac{\partial u}{\partial r} \to 0,\ T \to T_\infty,\ C \to C_\infty \text{as } r \to \infty. \tag{7}$$

The governing flow problem is reduced into ordinary differential equations by using the following transformations.

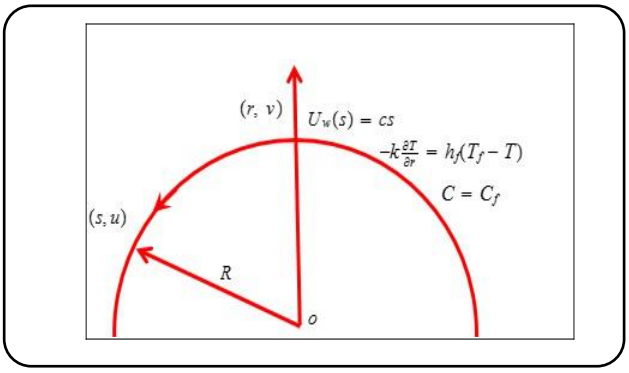

Fig. 1: Flow geometry.

$$u = U_w f'(\eta), \tag{8}$$

$$v = \frac{U_w R}{r+R} Re_b^{-\frac{1}{n+1}} \left[\frac{2n}{n+1} f(\eta) + \frac{1-n}{1+n} \eta f'(\eta)\right]$$

$$\psi = sU_w Re_b^{-\frac{1}{n+1}} f(\eta)$$

$$\theta(\eta) = \frac{T - T_\infty}{T_f - T_\infty}, \quad \phi(\eta) = \frac{C - C_\infty}{C_f - C_\infty}, \quad p = \rho a^2 s^2 P(\eta)$$

$$\eta = \frac{r}{s} Re_b^{\frac{1}{n+1}}$$

In order to incorporate the effect of thermal radiation, Rosseland [44] utilized the radiative heat flux on optically thick media and is defined as

$$q_r = -\frac{4\sigma^*}{3k^*}\frac{\partial T^4}{\partial r} \tag{9}$$

Under the assumption of temperature variances inside the flow are appropriately small, we may swell the term T^4 as a linear function of temperature in a Taylor series about T_∞ and disregarding the greater terms, one can get $T^4 = 3T_\infty^3 T - 3T_\infty^4$.

By plugging (8), Eq. (1) is identically satisfied and Eqs. (2) and (3) are taking the following form

$$\frac{\partial P}{\partial \eta} = \frac{f'^2}{\eta+K}, \tag{10}$$

$$\frac{2K}{\eta+K}P = \frac{K}{\eta+K}\left(\frac{2n}{n+1}\right)\left(ff'' + \frac{1}{\eta+K}ff'\right) - \tag{11}$$
$$\frac{K}{\eta+K}f'^2 + A\left[f''' + \frac{1}{\eta+K}f'' - \frac{1}{(\eta+K)^2}f'\right]$$
$$+n\left(f'' - \frac{1}{\eta+K}f'\right)^{n-1}\left(f''' - \frac{1}{\eta+K}f'' + \frac{1}{(\eta+K)^2}f'\right) +$$
$$\frac{2}{\eta+K}\left(f'' - \frac{1}{\eta+K}f'\right)^n + k_1(\theta + k_2\phi).$$

Substituting Eq. (10) into Eq. (9) by using Eq. (8) in Eqs. (4) to (7), we get the following form

$$A\left[f'''' + \frac{2}{\eta+K}f''' - \frac{1}{(\eta+K)^2}f'' + \frac{1}{(\eta+K)^3}f'\right] + \tag{12}$$
$$\left(\frac{2n}{n+1}\right)\left[\frac{K}{\eta+K}(ff''' + f'f'') + \frac{K}{(\eta+K)^2}(ff'' + f'^2) - \frac{K}{(\eta+K)^3}ff'\right]$$
$$-\frac{2K}{\eta+K}f'f'' - \frac{2K}{(\eta+K)^2}f'^2 +$$
$$n\left(f'' - \frac{1}{\eta+K}f'\right)^{n-1} \times$$
$$\left(f'''' + \frac{2}{\eta+K}f''' - \frac{1}{(\eta+K)^2}f'' + \frac{1}{(\eta+K)^3}f'\right)$$
$$+n(n-1)\left(f'' - \frac{1}{\eta+K}f'\right)^{n-2}\left(f''' - \frac{1}{\eta+K}f'' + \frac{1}{(\eta+K)^2}f'\right)^2$$
$$+2n\left(f'' - \frac{1}{\eta+K}f'\right)^{n-1}\left(\frac{1}{\eta+K}f'''' - \frac{1}{(\eta+K)^2}f'' + \frac{1}{(\eta+K)^3}f'\right)$$
$$+k_1\left(\theta' + \frac{\theta}{\eta+K} + k_2\left(\phi' + \frac{\phi}{\eta+K}\right)\right) = 0{,}12$$

$$(1+Rd)\left(\theta'' + \frac{\theta'}{\eta+K}\right) + \frac{\mathrm{Pr}K}{\eta+K}\left(\frac{2n}{n+1}\right)f\theta' + \frac{1}{\eta+K}\theta' = 0, \tag{13}$$

$$\phi'' + \frac{ScK}{\eta+K}\left(\frac{2n}{n+1}\right)f\phi' + \frac{1}{\eta+K}\theta' - RcSc\phi = 0, \tag{14}$$

$$f(0) = 0, \quad f'(0) = 1, \quad \theta'(0) = -\gamma_1(1 - \theta(0)), \tag{15}$$
$$\phi(0) = 1,$$

$$f' \to 0, \quad f'' \to 0, \quad \theta \to 0, \quad \phi \to 0 \quad \text{as} \quad \eta \to \infty. \tag{16}$$

All the flow parameters which lead the whole flow problem are listed below:

$Re_a = \frac{U_w s\rho}{a}$	$\alpha_1 = \frac{k}{\rho c_p}$
$Re_b = \frac{U_w{}^{2-n} s^n \rho}{b}$	$Pr = \frac{sU_w}{\alpha_1} Re_b^{-\frac{2}{n+1}}$
$A = \frac{Re_b^{\frac{2}{n+1}}}{Re_a}$	$Sc = \frac{sU_w}{D_B} Re_b^{-\frac{2}{n+1}}$
$k_1 = \frac{g\beta_T(T_f - T_\infty)/v^2}{(sU_w)^2/v^2}$	$Rd = \frac{16\sigma^* T^3{}_\infty}{3k^*}$
$k_2 = \frac{\beta_C(T_f - T_\infty)}{\beta_T(C_f - C_\infty)}$	$Rc = \frac{c\vartheta}{sU_w} Re_b^{\frac{2}{n+1}}$
$K = \frac{R}{s} Re_b^{\frac{1}{n+1}}$	$\gamma_1 = \frac{h_f}{k} sRe_b^{-\frac{1}{n+1}}$

The local skin friction coefficient, Nusselt number and Sherwood number are the physical quantities of interest and are defined by the following relations

Table 1: Comparison of bvp4c with shooting method, for different values of K when n = 3, A = 2.8 and $k_1 = k_2 = 0.1$.

Parameter	$-\frac{1}{2}\mathrm{Re}_b^{\frac{1}{n+1}} C_f$	$-\frac{1}{2}\mathrm{Re}_b^{\frac{1}{n+1}} C_f$
K	Bvp4c results	Shooting results
6	2.411551	2.411550
10	2.172554	2.172553
14	2.080998	2.080996
18	2.032922	2.032920

$$C_f = \frac{\tau_w}{1/2\,\rho U_w^2}, \quad Nu_s = \frac{q_w s}{k(T_f - T_\infty)}, \tag{17}$$

$$Sh_s = \frac{q_m s}{D_B(C_f - C_\infty)}$$

To obtain relation for local skin friction, Nusselt number and Sherwood number, we use the transformation defined in Eq. (8) in Eq. (16)

$$\frac{1}{2}Re_b^{\frac{1}{n+1}}C_f = A\left(f''(0) - \frac{1}{K}f'(0)\right) + \left(f''(0) - \frac{1}{K}f'(0)\right)^n, \tag{18}$$

$$Re_b^{-\frac{1}{n+1}}Nu_s = -(1 + Rd)\theta'(0), \tag{19}$$

$$Re_b^{-\frac{1}{n+1}}Sh_s = -\phi'(0). \tag{20}$$

METHODOLOGY VALIDATION

Problem under consideration for testing the impacts of different flow parameters is handled through numerical method. Specially, the effects of main governing flow parameters are presented in the form of graphs and tables. Moreover, the results obtained during the implementation of bvp4c are compared with the results obtained by shooting method [42]. All the outcomes are matched with each other as shown in Table 1. Present outcomes are further compared with previous published data by *Abbas et al.* [27] and *Sanni et al.* [29] in the limiting cases and as shown in Table 2.

RESULTS AND DISCUSSION

In order to incorporate the influence of mixed convection and chemical reaction phenomena on the flow of Sisko fluid in the presence of thermal radiation and convective conditions over a curved surface we made a numerical study. The highly non-linear problem given by Eqs. (12) to (14) subjected to boundary conditions (15) and (16) is considered for the elucidation in the form of graphs through bvp4c. All the flow parameters are tested in terms of flow pattern, velocity, temperature, concentration and prssure profiles. The drag forces, rate of heat and mass transfer are described with the help of local skin friction, Nusselt number and Sherwood number, respectively. All outcomes are presented with both the properties, i.e., shear-thinning and shear-thickening fluids. Like radius of curvature (K), the material parameter (A), mixed convection parameter (k_1), buoyancy ratio parameter (k_2), power-law index (n), Prandtl number (Pr), radiation parameter (Rd), Biot number (γ_1), chemical reaction parameter (Rc) and Schmidt number (Sc) are the parameters which govern the flow in curvilinear coordinates system.

Flow pattern

The impact of flow parameters on the flow pattern is illustrated through graph and is shown in Figs. 2(a,b). In this graph, both cases of shear thinning as well as shear thickening fluids are discussed. Where all the other flow parameters like $Re_b = 1000$, $c = 6$, $A = 3.8$, $K = 2$, $k_1 = k_2 = 0.3$ are kept fixed. The preceding Figs. show a non-uniform flow pattern near the curved surface and away from the curved surface the pattern is symmetric about the horizontal axis due to equal forces of buoyant flow. Through Figs. 3(a, b), a flow pattern is demonstrated for $K = 1000$ while keeping all other parameters fixed. Where this value of K shows almost a flat surface. A uniform flow pattern about the horizontal axis near the curved surface is reported, where the boundary layer depicts that the fluid particles are stretched away from the origin. Fig. 4(a) shows a flow pattern in the presence of mixed convection and buoyancy ratio parameter, when $n = 1$, $A = 0$ and $K = 5$. However, Fig. 4(b) represents a flow pattern in the absence of mixed convection and buoyancy parameter, when $n = 1$, $A = 0$ and $K = 5$. The flow pattern in both Figs. is portraying for Newtonian fluid and these display a uniform conduct near the curved surface as well as away from the curved surface. Near the curved surface the flow is stretched away from the slot and away from the curved surface a constant pattern is reported. Flow pattern represented in Fig. 5(a) is the influence of k_1 and k_2 while keeping the other parameters

Table 2: Comparison of the present work with previous results for different values of K when N = 1, A= 0 and $k_1 = k_2 = 0.1$

Parameter	$-\frac{1}{2}\mathrm{Re}_b^{\frac{1}{n+1}} C_f$	$-\frac{1}{2}\mathrm{Re}_b^{\frac{1}{n+1}} C_f$	$-\frac{1}{2}\mathrm{Re}_b^{\frac{1}{n+1}} C_f$
K	Present results	Abbas et al. [27]	Sanni et al. [29]
5	1.157641	1.1576	1.1576
10	1.073495	1.0735	1.0734
20	1.035613	1.0356	1.0355
30	1.023533	1.023	1.0235
40	1.017587	1.0176	1.0176
50	1.014049	1.0141	1.140
100	1.007039	1.0070	1.0070
200	1.003564	1.0036	1.0036
1000	1.000799	1.0008	1.0008
∞	1.000179	1.0000	1.0000

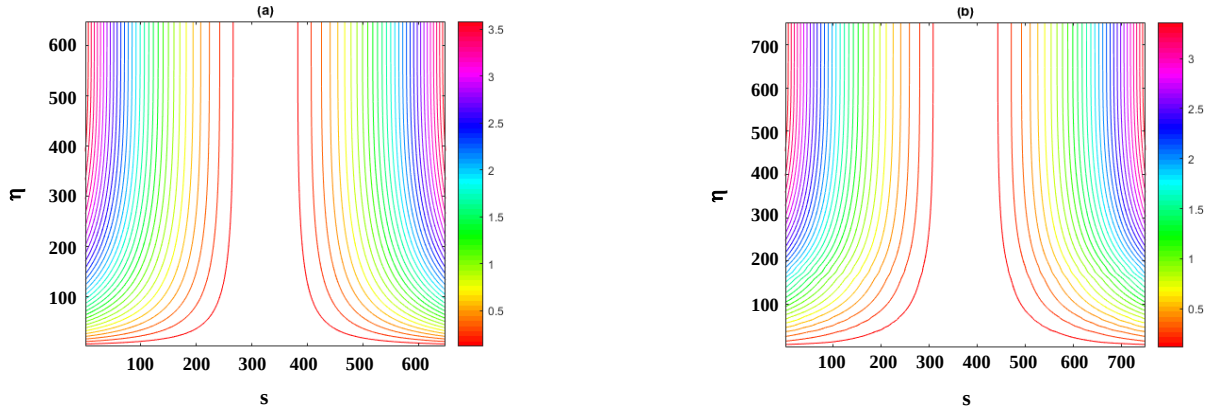

Fig. 2: Streamlines pattern for (a) n = 0.8 and (b) n = 1.8 when K=2.

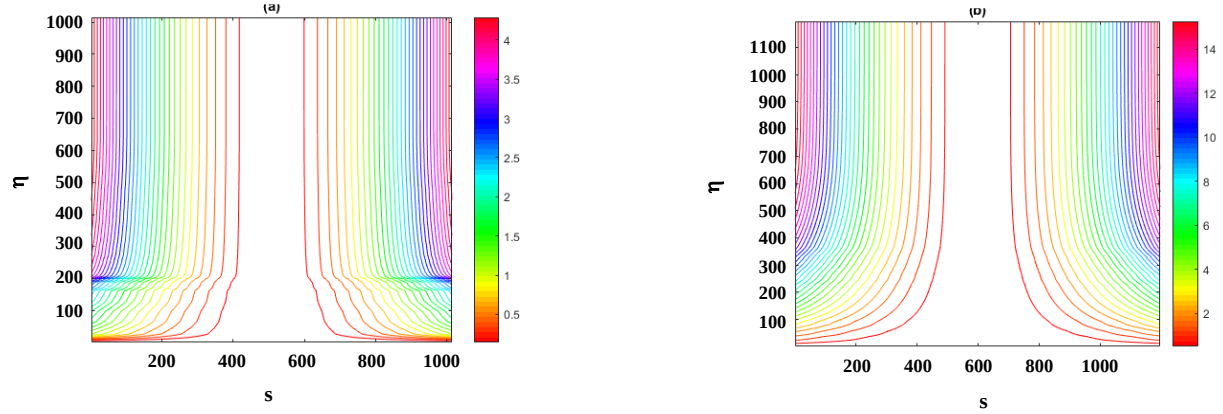

Fig. 3: Streamlines pattern for (a) n = 0.8 and (b)n = 1.8 when K = 10000.

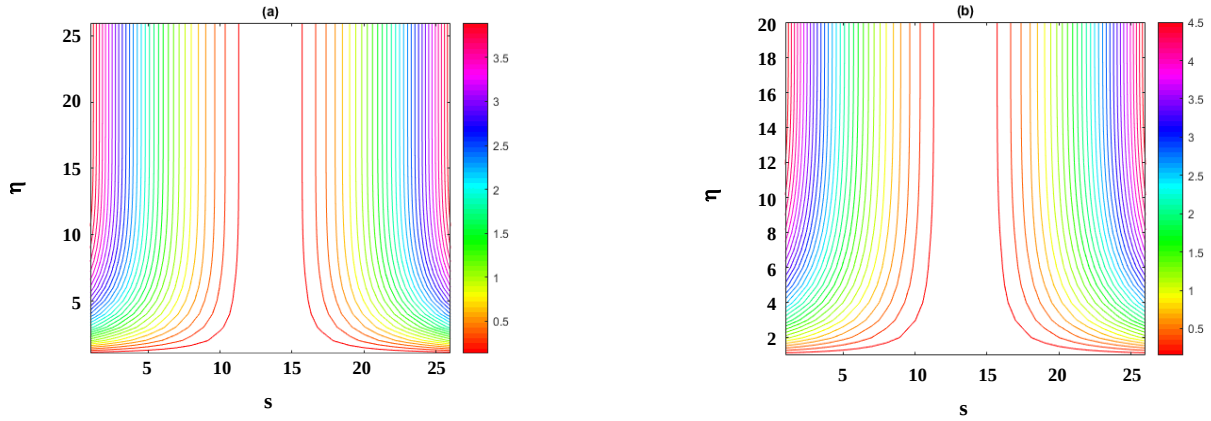

Fig. 4: Streamlines pattern for (a) $k_1 = k_2 = 0.3$ (b) $k_1 = k_2 = 0.0$ when n=1, A= 0 and K = 5.

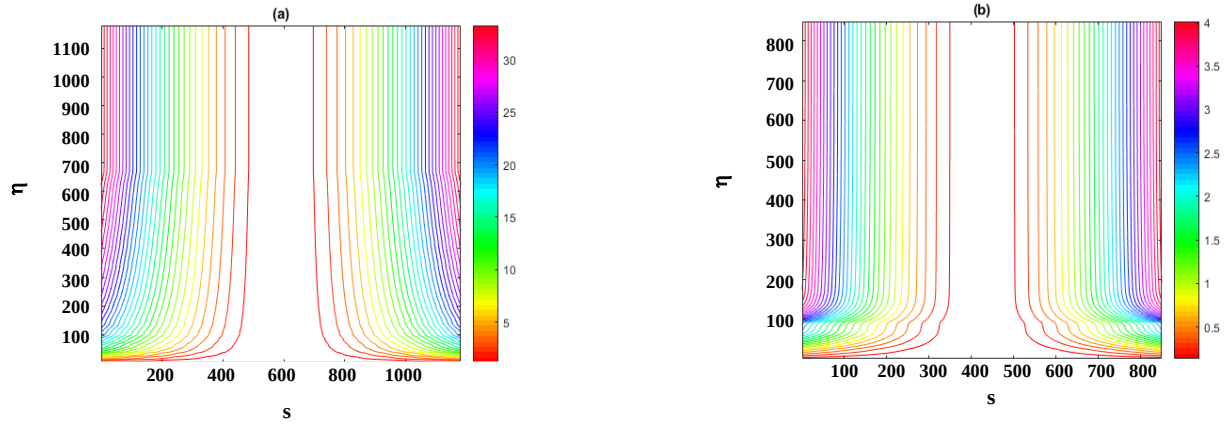

Fig. 5: Streamlines pattern for (a) n = 2, A = 0 and $k_1 = k_2 = 0.3$ (b) n = 0.8, A = 3.8 and $k_1 = k_2 = 0.0$ when K = 5.

fixed, likely when $n = 2$, $A = 0$ and $k_1 = k_2 = 0.3$. Here a very small portion of the flow pattern contributing in the laminar boundary layer, i.e., the stretched flow away from the slot carrying a very little portion. Also the flow is symmetric about the horizontal axis. From Fig. 5(b), we concluded that for shear thinning fluid, the flow pattern near the stretched surface illustrates a remarkable conduct and the flow is symmetric about horizontal axis.

Velocity profile

The influence of A and K on $f'(\eta)$ is demonstrated through Figs. 6(a-d). The impact of increasing values of A on $f'(\eta)$ is reported in escalation conduct for shear thinning as well as shear thickening fluids. As a result the boundary layer thickness also increases in both cases. Additionally, the effect of A in the shear thickening case are more prominent as compared to the shear thinning case. In the aforementioned Fig., effect of increasing values of K is noticed in escalating conduct for pseudoplastic as well as dilatant fluids. But the result is very prominent in case of pseudoplastic fluid. Physically, the growing values of K shows that the curved surface is going to reduce to the planner sheet. Where the velocity of the fluid is almost higher than the velocity of fluid at the curved surface. An increasing behavior for both shear thining and shear thickening fluids is observed for growing values of k_1 through Figs. 7(a, b). In physical point of view, growing values of k_1 rises the buoyancy forces and as a result increases gravity due to which velocity the fluid enriches. Again an uplifting effect of $f'(\eta)$ is also reported with the increasing values of k_2 and is presented through Fig. 7(c, d), while testing both properties, i.e., shear thinning as well as shear thickening fluids. This is due to an increase in the concentration of buoyancy force via higher values of k_2 yields higher viscosity. The results are very significant in case of shear thinning fluid.

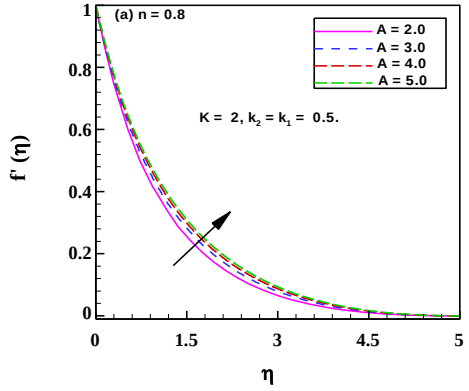

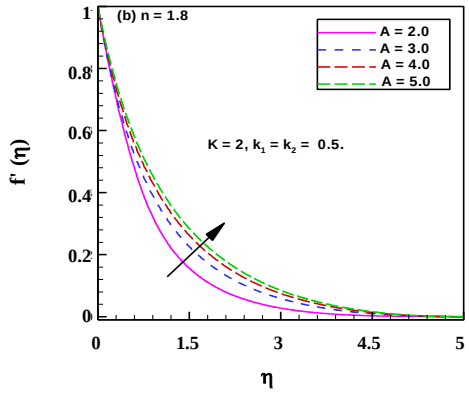

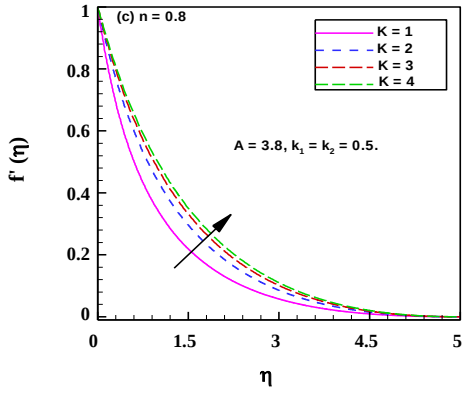

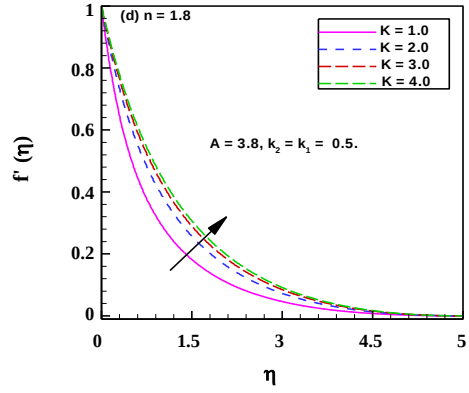

Fig. 6: Influence of A and K on f'(η).

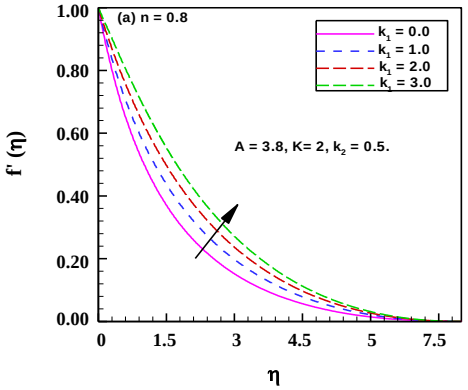

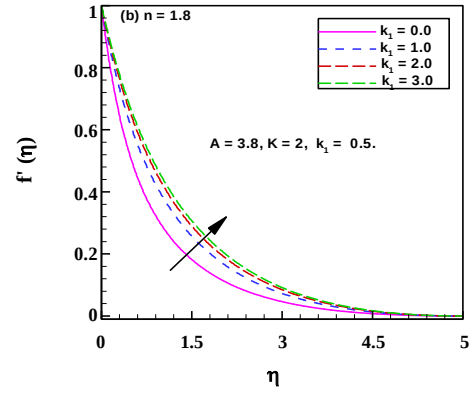

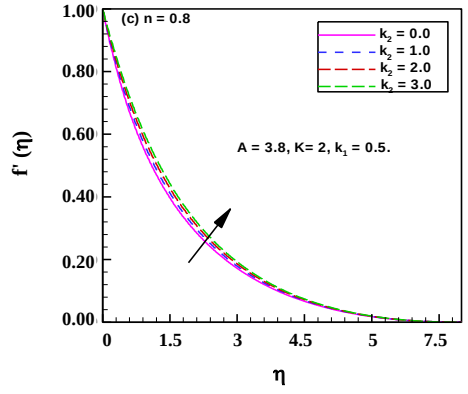

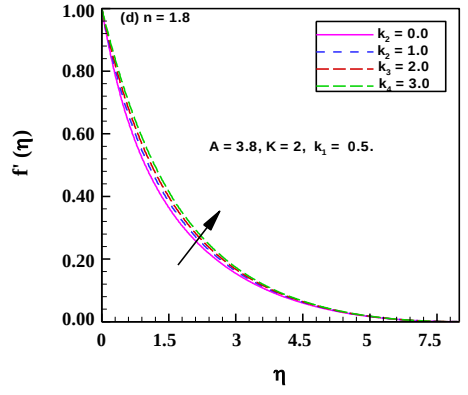

Fig. 7: Influence of k_1 and k_2 on f'(η).

The associated boundary layer thickness also increases with increasing values of these parameters.

Temperature profile

To describe the impacts of A and K on $\theta(\eta)$, we have plotted Figs. 8(a-d). All these Figs. depict a diminishing conduct while increasing values of A and K. The shear thinning and shear thickening fluids charactiristics are studied in all four graphs of $\theta(\eta)$. Physically, for growing values of A, the temperature of the fluid reduces due to high shear rate causesing low viscosity. On the other hand for growing values of K physically tells about the increment in velocity and as a result the fluid particles are move away from each other and this is why the temperature of the fluid decreases.

In Fig. 9(a, b), the decreasing effect of increasing values of k_1 on $\theta(\eta)$ is observed for shear thinning as well as shear thickening fluids. Physically, for increasing values of k_1, the buoyancy forces are higher which increases the gravity and which leads to the declining effect in temperatuer of the fluid along with thermal boundary layer thickness. A diminishing behavior of $\theta(\eta)$ for shear thinning and shear thickening fluids *via* intensifying values of k_2 is investigated through Fig. 9(c, d). Physically, with growing behavior of concentration buoyancy forces yields a higher viscosity. A close view of Figs. 8 and 9 reveal that the boundary layer thickness is higher in case of shear thinning fluid as compared to the shear thicknening fluid. Increasing values of Rd and γ_1 for $(0 < n < 1)$ and $(n > 1)$ are responsible for larger $\theta(\eta)$ and associated thermal boundary layer thickness as shown in Figs. 10(a-d). Physically, radiation rises the temperature of the fluid. On the other hand the augmented values of γ_1 causes an enhancement in convection and as a result the resistance of thermal sheet is reduced.

Concentration profile

The depiction of K is measured through Figs. 11(a, b). An uplifting influence of this parameter on $\phi(\eta)$ is plotted in the presence of shear thinning and shear thickening conditions. The curvature parameter enhances the concentration profile and associated concentration boundary layer thickness in shear thinning fluid. However, an opposite trend is noticed for shear thickening fluid. On other hand, for larger values of mixed convection parameter k_1, reduction in the concentration of the fluid

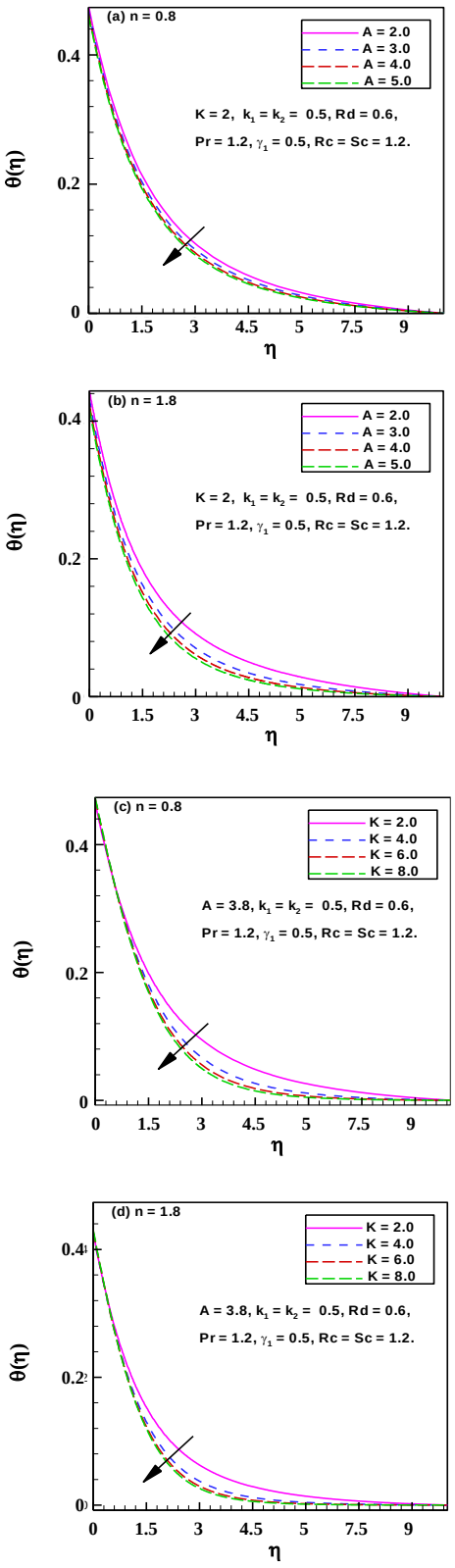

Fig. 8: Influence of A and K on θ(η).

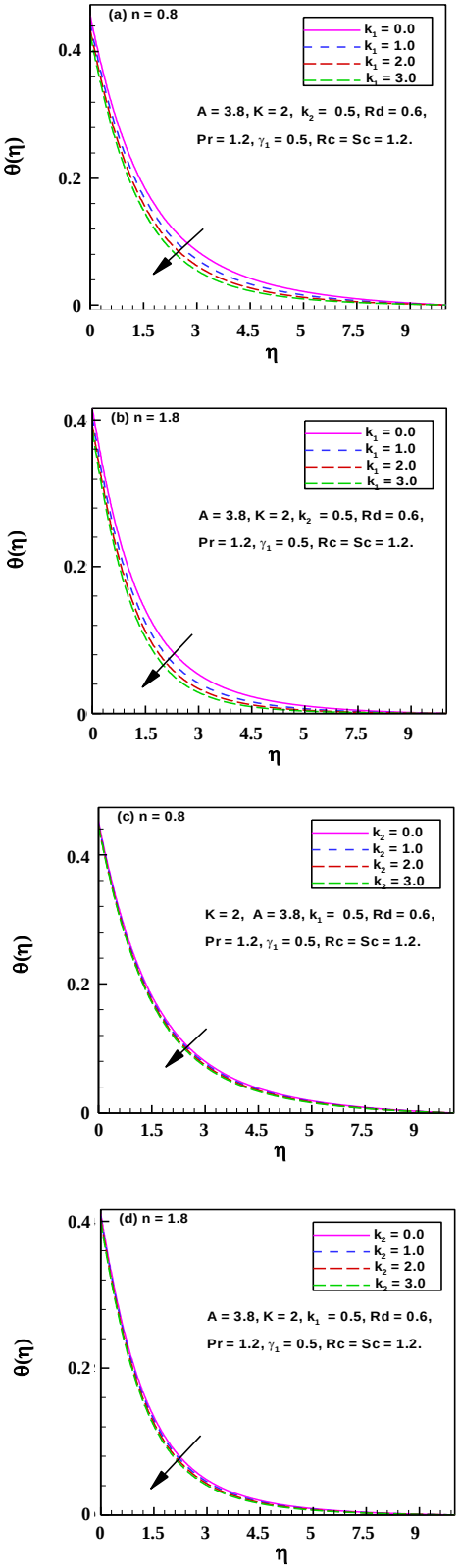

Fig. 9: Influence of k_1 and k_2 on $\theta(\eta)$.

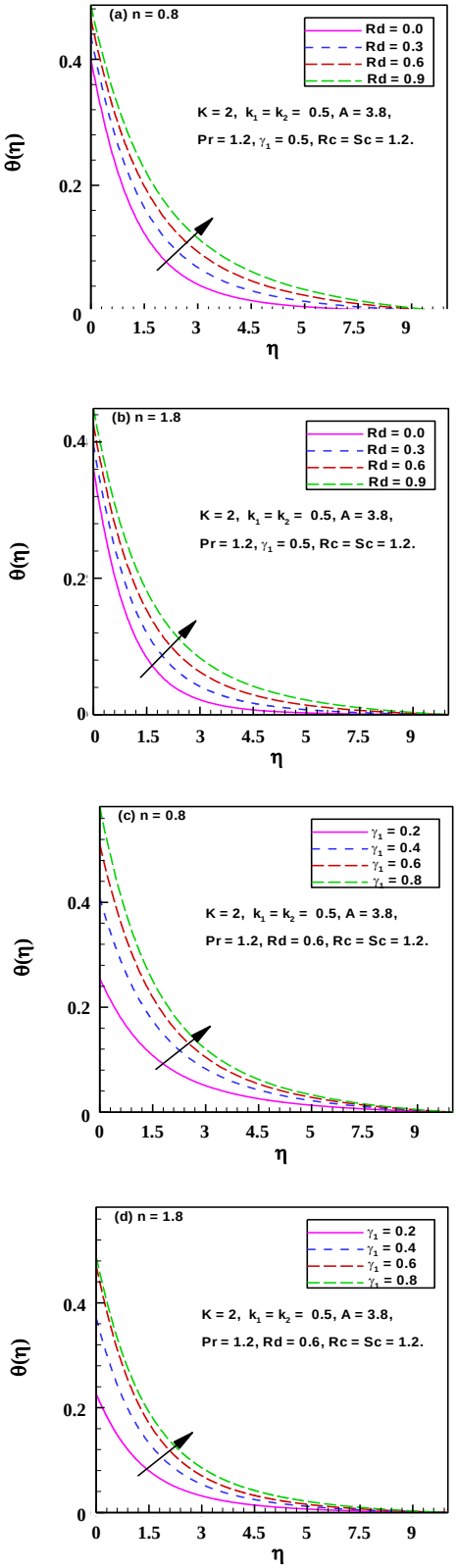

Fig. 10: Influence of Rd and γ_1 on $\theta(\eta)$.

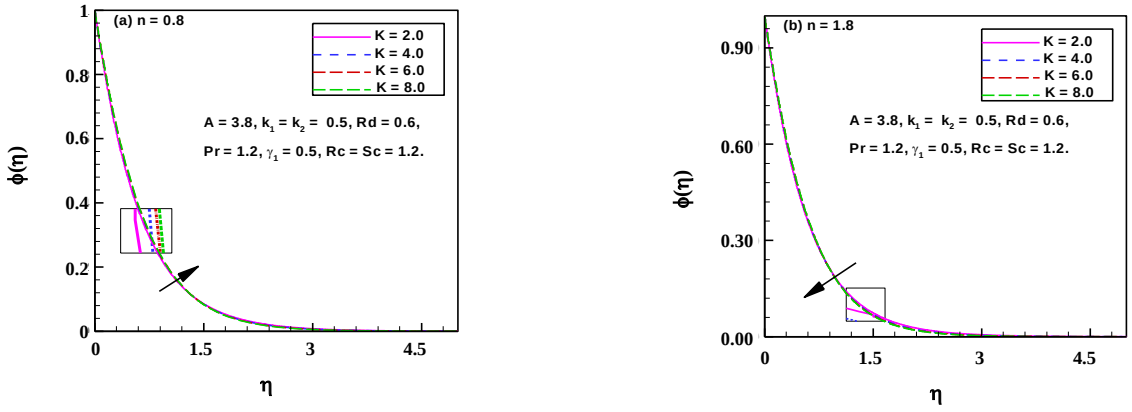

Fig. 11: Influence of K on $\phi(\eta)$.

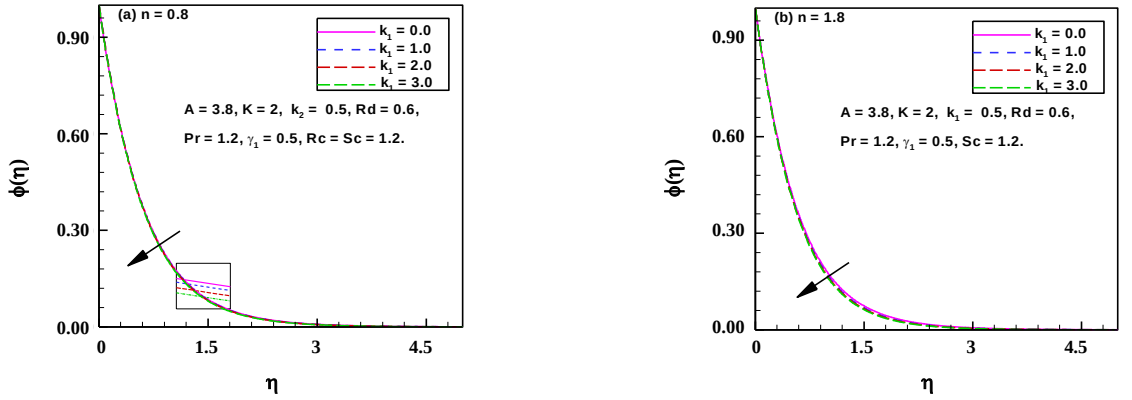

Fig. 12: Influence of k_1 on $\phi(\eta)$.

is noticed for both cases as shown in Figs. 12(a, b). From physical point of view, the decrease in concentration is due to encouraging pressure gradient and which is because of the action of buoyancy forces. Thus larger buoyancy forces backings in upward direction and as a result $\phi(\eta)$ is declining. Figs. 13(a, b) presents the impacts of Rc on $\phi(\eta)$ with shear thinning and shear thickening fluids property. A meaningful diminishing demeanors are detected with the variation of aforesaid parameter. Physically, when $(Rc > 0)$ shows a destruction in chemical reaction and for $(Rc < 0)$ the chemical reaction is generative. Additionally, the concentration is reduce in case of destructive chemical reaction while it increases in case of generative chemical reaction. The associated boundary layer thickness also reduces in the case of destruction of chemical reaction.

Pressure profile

The effect of decreasing values of curvature parameter on the magnitude of $P(\eta)$ inside the boundary layer is detected in enhancing conduct and is shown in Fig. 14(a, b) for Sisko fluid and Newtonian fluids, respectively. It can be described on the foundation of curvilinear nature of the surface. Rising the curvature of the curved surface which causes secondary flow under the action of centrifugal force and due to this action the fluid particles directed toward the curved path along the surface of the sheet. Yet, the pressure tends to zero far from the boundary. This is because of the fact that as we travel away from the boundary the stream lines of the flow conduct in the same way as they do in the flow past a planner sheet. However, near to the curved surface the magnitude of the pressure is growing function of reducing values of K. Here give a comparison between Sisko and Newtonian fluids. Through Fig. 14(c) a growing manner in the magnitude of $P(\eta)$ is due to the diminishing values of A. Physical reasoning about the reducing values of A tells us about the reduction in the viscosity of fluid which causes growth in the shear rate of the fluid flow. Fig. 14(d) shows the increasing

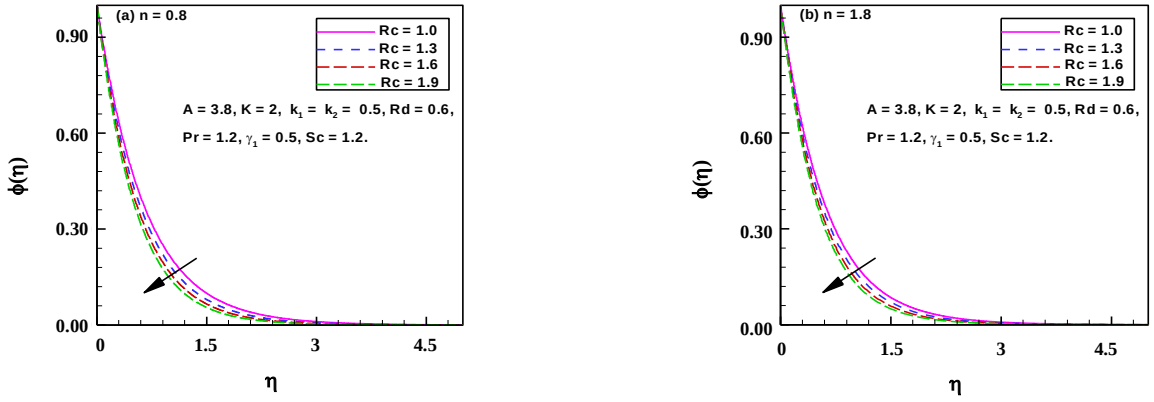

Fig. 13: Influence of Rc on $\phi(\eta)$.

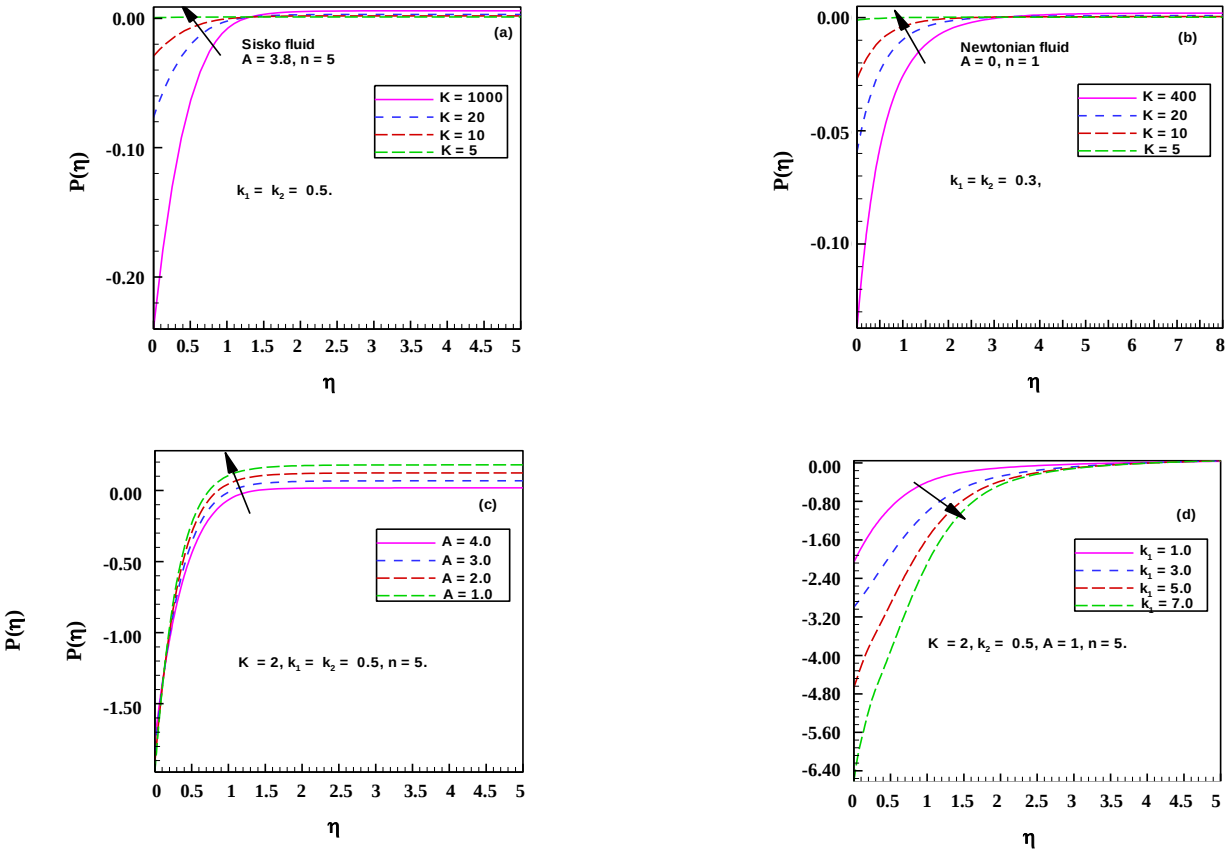

Fig. 14: Influence of A and k_1 on $P(\eta)$.

variation in the magnitude of $P(\eta)$ inside the boundary layer and this is because of increasing values of mixed convection parameter k_1. Physical reasoning behind this phenomenon is that k_1 enhances the buoyancy forces and which uplifting the gravity due which the magnitude of the pressure inside the boundary layer escalated.

Local skin friction, Nusselt and Sherwood numbers

Figs. 15(a, b) are illustrated to describe the features of the resistive forces. In these graphs, the skin friction with the influence of K and k_1 via A is plotted. The skin friction shows a declining conduct for the said increasing parameters values. The effect of increasing radiation

Table 3: Local Nusselt and Sherwood numbers for different values of K, Pr, Sc when n = 0.8, A = 3.8, $\gamma_1 \to \infty$ and $k_1 = k_2 = Rd = Rc = 0$.

K	Pr	$-\theta'(0)$	K	Sc	$-\varphi'(0)$
2	1.2	0.7702742	2		0.7703336
4		0.7589168	4		0.7589168
6		0.7519532	6		0.7520098
2	1.0	0.6987988	2	1.0	0.6988478
	1.2	0.7702742		1.2	0.7703336
	1.4	0.8365209		1.4	0.8365909

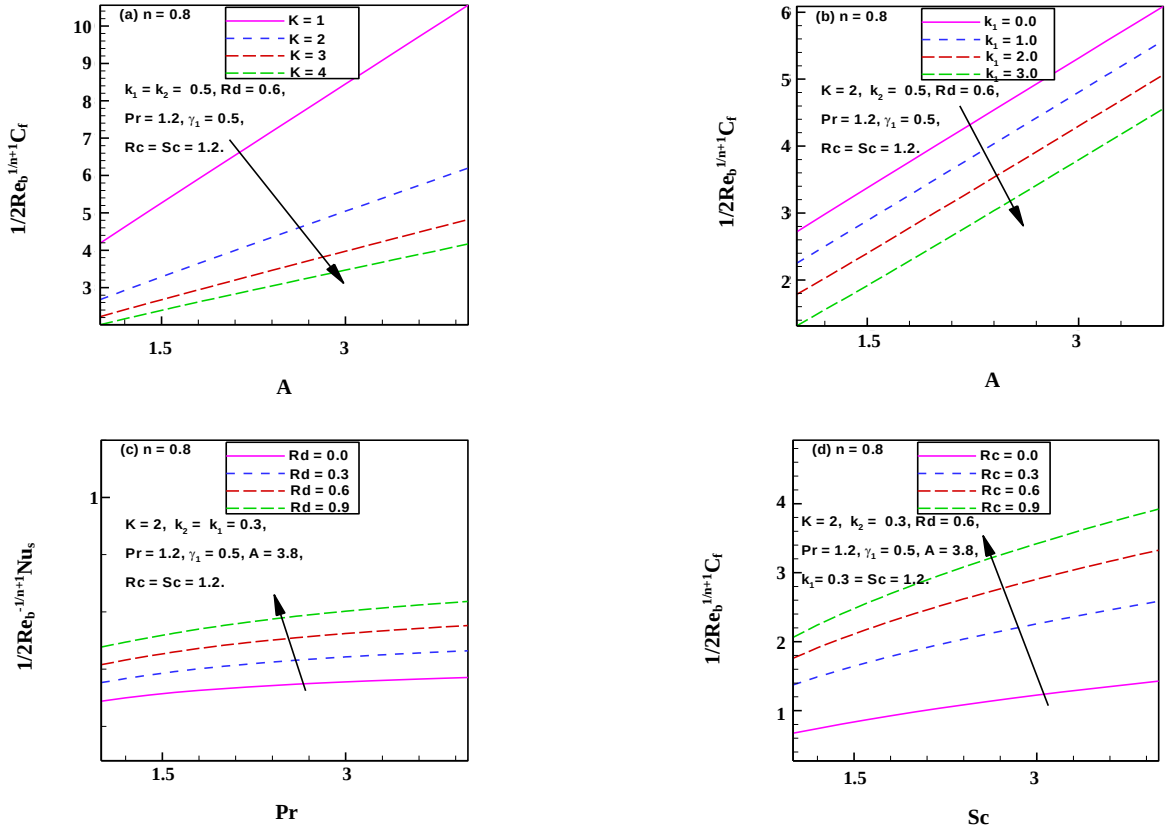

Fig. 15: Influence of K, k_1 , Rd and Rc on skin friction, Nusselt number and Sherwood number.

parameter is tested in the graph of Nusselt number via Pr and is shown in Fig. 15(c). This influence is detected in the growing conduct. The rate of mass transfer is further demonstrated through Fig. 15(d), where an increase in Rc causes the enhancment in the mass transfer rate via Sc. The local Nusselt and Sherwood number is computed and presented through Table 3 with increasing conduct for increasing values of curvature parameter and an opposite trend is observed for Prandtl and Schmidt number, repectively.

CONCLUSIONS

The effects of mixed convection, thermal radiation, chemical reaction and convective boundary conditions on the radiative flow of Sisko fluid over a curved surface was explored in this work. All the outcomes are expressed in the form of velocity, temperature, concentration and pressure graphs. The outcomes were also validated through another numerical method namely shooting method as well as with the previous published works.

Main findings of the present study are illustrated in the following paragraph.

The mixed convection and buoyancy parameters enhanced the velocity of the shear thinning as well as shear thickening fluids flow. On the other hand, a reverse trend was observed with plotting of temperature of fluid with effects of same parameters. The radiation parameter and Biot number uplifted the temperature of the fluid with shear-thickening as well as shear thinning property. A reduction in concentration of the fluid was noticed with the impact of mixed convection and chemical reaction parameter with pseudoplastic as well as dilatant fluids property. Magnitude of the pressure inside the boundary layer was increasing function of mixed convection parameter. However, for higher values of material parameter, the magnitude of pressure inside the boundary layer was noticed in decreasing order. The skin friction was reducing during the uplifting values of mixed convection parameter via material parameter. The skin frcition graphs against material parameter was noticed in declined order for higher values of curvature parameter. Enrichment in the rate of heat and mass transfer via Prandtl and Schmidt number was found as an increasing function of radiation and chemical reaction parameters. The tabular values of rate of heat and mass transfer for increasing values of curvature parameter was noticed in declining trend while an opposite behavior was noticed for Prandtl and Schmidth number, respectively.

Nomenclature

r,s	Curvilinear coordinates
(a,b,n)	Material constants
R	Radius of curvature
V	Velocity vector
u,v	Velocity components
f	Dimensionless stream function
q_w,q_m	The wall heat and mass fluxes
k	Thermal conductivity
T	Temperature of fluid
T_w	Temperature at the wall
T_∞	Ambient temperature
C	Nanoparticle volume friction
C_w	Concentration at the wall
C_∞	Ambient concentration
q_r	Radiative heat flux
σ^*	Stefan-Boltzman constant
k^*	Mean absorption coefficient
ψ	Stream function
θ	Dimensionless temperature
φ	Dimensionless concentration
A_1	First Rivlin Erickson Tensor
c	Constant
β_T	Thermal expansion coefficient
B_C	Solutal expansion coefficient
c_p	Specific heat
α_1	Thermal diffusivity
p	Denotes the pressure
τ	Cauchy stress tensor
τ_w	Surface shear stress
ρ	Fluid density
η	Dimensionless variable
γ_1	Biot number
I	Identity tensor
S	The extra stress tensor
C_f	Skin friction coefficient
Nu_s	Nusselt number
Sh_s	Sherwood number
Re_a,Re_b	Local Reynolds numbers
A	Material parameter of the Sisko fluid
K	Dimensionless radius of curvature
ϑ	First order chemical reaction parameter
Rc	Chemical reaction parameter
Pr	Prandtl number
Sc	Schmidt number
k_1	Mixed convection parameter
k_2	Buoyancy ratio parameter
ν	Kinematic viscosity
h_f	Coefficient of heat transfer

Received : Nov. 20, 2018 ; Accepted :Mar. 21, 2019

REFERENCES

[1] Seddeek M.A., Abdel A.M., Effects Of Radiation And Thermal Diffusivity on Heat Transfer Over a Stretching Surface with Variable Heat Flux, *Phys. Lett. A*, 348: 172—179 (2006).

[2] Hayat T., Khan M.I., Farooq M., Alsaedi A., Waqas M., Yasmeen T., Impact of Cattaneo-Christov Heat Flux Model In Flow of Variable Thermal Conductivity Fluid over A Variable Thicked Surface, *Int. J. Heat Mass Transf.*, **99**: 702—710 (2016).

[3] Hayat T., Khan M.I., Farooq M., Yasmeen T., Alsaedi A., Stagnation Point Flow with Cattaneo-Christov Heat Flux and Homogeneous-Heterogeneous Reactions, *J. Mol. Liq.*, **220**: 49--55 (2016).

[4] Hayat T., Khan M.I., Waqas M., Alsaedi A., Farooq M., Numerical Simulation for Melting Heat Transfer and Radiation Effects In Stagnation Point Flow of Carbon-- Water Nanofluid, *Comput. Meth. Appl. Mech. Eng.*, **315**: 1011-1024 (2017).

[5] Yasmeen T., Hayat T., Khan M.I., Imtiaz M., Alsaedi A., Ferrofluid Flow by a Stretched Surface in the Presence of Magnetic Dipole and Homogeneous-Heterogeneous Reactions, *J. Mol. Liq.*, **223**: 1000-1005 (2016).

[6] Krishnamurthy M.R., Gireesha B.J., Prasannakumara B.C., Gorla R.S.R., Thermal Radiation and Chemical Reaction Effects on Boundary Layer Slip Flow and Melting Heat Transfer Of Nanofluid Induced by a Nonlinear Stretching Sheet, *Nonlinear Eng.*, **5**(3): 147-159 (2016).

[7] Motsumi T.G., Makinde O.D., Effects of Thermal Radiation and Viscous Dissipation on Boundary Layer Flow of Nanofluids over a Permeable Moving Flat Plate, *Physica Scripta*, **86**: 1-11 (2012).

[8] Hayat T., Ullah I., Muhammad T., Alsaedi A., Radiative Three-Dimensional Flow with Soret and Dufour Effects, *Int. J. Mech. Sci.*, **133**: 829-837 (2017).

[9] Hassan A.R., Maritz R.., Gbadeyan J.A., A Reactive Hydromagnetic Heat Generating Fluid Flow with Thermal Radiation Within Porous Channel with Symmetrical Convective Cooling, *Int. J. Therm. Sci.*, **122**: 248-256 (2017).

[10] Sparrow E.M., Combined Forced and Free Convection in a Boundary Layer Flow, *Phys. Fluids*, **2**: 319(1959).

[11] Zhou X., Huai X., Numerical Investigation of Thermocapillary Convection in a Liquid Layer with Free Surface, *Microgravity Sci. Tech.*, **25**: 335-341 (2014).

[12] Lyubimova T., Beysens D., Gandikota G., Amiroudine S., Vibration Effect on A Thermal Front Propagation in a Square Cavity Filled with Incompressible Fluid, *Microgravity Sci. Tech.*, **26**: 51-56 (2014).

[13] Munro T.R., Ban H., Flow and Heat Flux Behavior of Micro-Bubble Jet Flows Observed in Thin, Twisted-Wire, Subcooled Boiling in Microgravity, *Microgravity Sci. Tech.*, **27**: 49-60 (2015).

[14] Chen Jie-C., Zhang L., You-Rong Yu Jia-J., Three-Dimensional Numerical Simulation of Pure Solutocapillary Flow in a Shallow Annular Pool For Mixture Fluid with High Schmidt Number, *Microgravity Sci. Tech.*, **28**(1): 49-57 (2016).

[15] Lei Y., Chen Z., Shi J., Analysis of Condensation Heat Transfer Performance in Curved Triangle Microchannels Based on the Volume of Fluid Method, *Microgravity Sci. Tech.*, **29**: 433-443 (2017).

[16] Merkin J.H., Pop I., Mixed Convection Along a Vertical Surface: Similarity Solutions for Uniform Flow, *Fluid Dyn. Res.*, **30**(4): 233-250 (2002).

[17] Nadeem S., Saleem S., Mixed Convection Flow of Eyring--Powell Fluid Along a Rotating Cone, *Results Phys.*, **4**: 54-62 (2014).

[18] Noor N.F.M., Haq R.U., Nadeem S., Mixed Convection Stagnation Flow of a Micropolar Nanofluid Along a Vertically Stretching Surface with Slip Effects, *Meccanica*, **50**(8): 2007-2022 (2015).

[19] Haq R.U., Hamouch Z., Hussain S.T., Mekkaoui T., MHD Mixed Convection Flow Along a Vertically Heated Sheet, *Int. J. Hydrogen Energy*, **42**(24): 15925-15932 (2017).

[20] Turkyilmazoglu M., Mixed Convection Flow of Magnetohydrodynamic Micropolar Fluid Due to a Porous Heated/Cooled Deformable Plate: Exact Solutions, *Int. J. Heat Mass Transf.*, **106**: 127-134 (2017).

[21] Turkyilmazoglu M., Analytical Solutions to Mixed Convection MHD Fluid Flow Induced by a Nonlinearly Deforming Permeable Surface, *Commun. Nonlinear Sci. Numer. Simul.*, **63**: 373-379 (2018).

[22] Hayat T., Shah F., Khan .I., Alsaedi A., Yasmeen T., Modeling MHD Stagnation Point Flow of Thixotropic Fluid with Non-Uniform Heat Absorption/Generation, *Microgravity Sci. Tech.*, **29**: 459-465 (2017).

[23] Crane L.J., Flow Past a Stretching Plate, *J. Appl. Math. Phys., (ZAMP)* **21**: 645-647 (1970).

[24] Khan Y., Abdou M.A., Faraz N., Nildirim A., Wu Q., Numerical Solution of MHD Flow over a Nonlinear Porous Stretching Sheet, *Iran. J. Chem. Chem. Eng. (IJCCE)*, **31**(3): 125-132 (2012).

[25] Turkyilmazoglu M., Equivalences and Correspondences Between the Deforming Body Induced Flow and Heat in Two-Three Dimensions, *Phys. Fluids*, **28**: 043102 (2016).

[26] Sajid M., Ali N., Javed T., Abbas Z., Stretching a Curved Surface in a Viscous Fluid, *Chinese Phys. Lett.*, **27**: 024703 (2010).

[27] Abbas Z., Naveed M., Sajid M., Heat Transfer Analysis for Stretching Flow over a Curved Surface with Magnetic Field, *J. Eng. Thermophys.*, **22**: 337-345 (2013).

[28] Rosca N.C., Pop I., Unsteady Boundary Layer Flow over a Permeable Curved Stretching/Shrinking Surface, *Europ. J. Mech. - B/Fluids*, **51**: 61-67 (2015).

[29] Sanni K.M., Asghar S., Jalil M., Okechi N.F., Flow of Viscous Fluid Along a Nonlinearly Stretching Curved Surface, *Results Phys.*, **7**: 1-4(2017).

[30] Labropulu F., Li D., Pop I., Non-Orthogonal Stagnation-Point Flow Towards A Stretching Surface in a Non-Newtonian Fluid With Heat Transfer, *Int. J. Thermal Sci.*, **49**(6): 1042-1050 (2010).

[31] Nadeem S., Akram S., Akbar N., Simulation of Heat and Chemical Reactions on Peristaltic Flow of a Williamson Fluid in an Inclined Asymmetric Channel, *Iran. J. Chem. Chem. Eng. (IJCCE)*, **32**(2): 93-107 (2013).

[32] Hayat T., Ali S., Awais M., Alhuthali M.S., Newtonian Heating In Stagnation Point Flow of Burgers Fluid, *Appl. Math. Mech. -Engl. Ed.*, **36**(1): 61-68 (2015).

[33] Hayat T., Ali S., Asif M.F., Alsaedi A., On Comparison of Series And Numerical Solutions for Flow of Eyring-Powell Fluid with Newtonian Heating and Internal Heat Generation/Absorption, *PLOS ONE*, **10**: 1-13 (2015).

[34] Hayat T., Ali S., Alsaedi A., Alsulami H.H., Influence of Thermal Radiation and Joule Heating in the Eyring-Powell Fluid Flow with the Soret and Dufour Effects, *J. Appl. Mech. Tech. Phys.*, **57**(6): 1051-1060 (2016).

[35] Madhu M., Kishan N., Finite Element Analysis of Heat and Mass Transfer by MHD Mixed Convection Stagnation-Point Flow of a Non-Newtonian Power-Law Nanofluid Towards a Stretching Surface with Radiation, *J. Egyptian Math. Soci.*, **24**(3): 458-470 (2016).

[36] Akram S., Nadeem S., Influence Of Nanoparticles Phenomena on The Peristaltic Flow of Pseudoplastic Fluid in an Inclined Asymmetric Channel with Different Wave Forms, *Iran. J. Chem. Chem. Eng. (IJCCE)*, **36**(2): 107-124 (2017).

[37] Farooq A., Ali R., Benim A.C., Soret and Dufour Effects on Three Dimensional Oldroyd-B Fluid, *Physica A*, **503**: 345-354 (2018).

[38] Malik R., Khan M., Munir A., Khan W.A., Flow and Heat Transfer in Sisko Fluid with Convective Boundary Condition, *PLOS ONE*, **9**(10): E107989 (2014).

[39] Khan M., Ahmad L., Alshomrani A.A., Alzahrani A.K., Alghamdi M.S., A 3D Sisko Fluid Flow with Cattaneo-Christov Heat Flux Model and Heterogeneous-Homogeneous Reactions: a Numerical Study, *J. Mol. Liq.*, **238**: 19-26 (2017).

[40] Khan M., Ahmad L., Khan W.A., Numerically Framing The Impact of Radiation on Magnetonanoparticles for 3D Sisko Fluid Fow, *J. Braz. Soc. Mech. Sci. Eng.*, **39**: 4475-4487 (2017).

[41] Ahmad L., Khan M., Khan W.A., Numerical Investigation of Magneto-Nanoparticles for Unsteady 3D Generalized Newtonian Liquid Flow, *Europ. Phys. J. Plus*, **9**(132): 373 (2017).

[42] Malik R., Khan M., Numerical Study of Homogeneous-Heterogeneous Reactions in Sisko Fluid Flow Past a/ Stretching Cylinder, *Results Phys.*, **8**: 64-70 (2018).

[43] Ahmad L., Khan M., Numerical Simulation for MHD Flow of Sisko Nanofluid over a Moving Curved Surface: a Revised Model, *Microsystem Tech.*, (2018): https://Doi.Org/10.1007/S00542-018-4128-3.

[44] Rosseland S., "Astrophysik und Atom-Theoretische Grundlagen", *Springer-Verlag, Berlin*, 41-44 (1931).